Measurements of Fluctuating Air Loads on a Circular Cylinder

L. V. SCHMIDT*
California Institute of Technology, Pasadena, Calif.

Measurements were made of the unsteady air loads, both lift and drag, developed on a circular cylinder when exposed to flow normal to the axis of symmetry in the supercritical Reynolds number range from 0.38×10^6 to 0.75×10^6. The three-dimensional nature of the flow, which is a consequence of the separated viscous flow, is recognized. A statistical description of the spatially varying random-type air loads is provided by cross-spectral densities and cross-correlation coefficients. Information of this type, when defined in detail, has application to the response problem of a cylindrical structure that is exposed to air loads. An unusual trait that was observed was the extreme sensitivity of the flow to surface irregularities in the supercritical Reynolds number region. In addition to an influence upon the local and spatial character of the fluctuating loads, steady-state values of local lift could be induced by suitably orienting surface disturbances on the forward portion of the cylinder.

Nomenclature

C_L = local lift force coefficient = (lift force/unit span)/qD
C_D = local drag force coefficient = (drag force/unit span)/qD
D = cylinder diameter
f = frequency, cps
q = dynamic pressure, $q = \frac{1}{2}\rho V^2$
t = time
R = Reynolds number of cylinder = VD/ν
S = Strouhal number = fD/V
V = velocity of undisturbed flow
x = axial coordinate along cylinder axis, $x = 0$ at base
ρ = mass density of fluid
ν = kinematic viscosity of fluid
τ = time lag
θ = angular coordinate for cylinder surface, zero reference is forward stagnation point
ϕ = power spectral density
Φ = cospectral density, real part of cross spectra
Ψ = quadspectral density, imaginary part of cross spectra
χ = correlation length, dimensionless
$R_{(\ )}$ = cross-correlation coefficient, subscript denotes load station orientation

1. Introduction

A CIRCULAR cylinder, when placed normal to an airstream, experiences unsteady lift and drag loads as a result of the fluctuating pressures acting on the cylinder. These effects, which occur whether the cylinder is vibrating or stationary, have considerable practical interest both in engineering and fluid mechanics.

The knowledge of the unsteady loads in the supercritical Reynolds number flow regions has engineering application to current problems of import dealing with the response of large cylindrical bodies such as smokestacks and missiles when exposed to surface winds. The fluid mechanics interest is clear since the problem is intimately associated with the problem of vortex shedding, for which there is still no suitable theoretical treatment. The literature background for the over-all problem has been presented by Fung[1, 2] in 1958. The literature on the closely allied subject of vortex shedding is quite extensive, with notable reviews being given by Goldstein[3] in 1938, Rosenhead[4] in 1953, and Humphreys[5] in 1959.

The vortex shedding phenomena can be classified in terms of the cylinder Reynolds number R into a subcritical and a supercritical region with a transition zone occurring in the range of $2 \times 10^5 < R < 5 \times 10^5$. In the subcritical region, the character of the wake is predominantly periodic, and is associated with a laminar-type flow separation. Roshko[6] reported in 1960 that the supercritical flow region is characterized by a turbulent wake without any dominant frequencies for Reynolds numbers below about 3×10^6. Periodicity was observed when R was greater than approximately 3×10^6.

The unsteady loads can also be described according to flow ranges. Based on observations made in the subcritical Reynolds number range (e.g., Macovsky[7] and Keefe[8]), it has been found that the unsteady lift load is of the same order of magnitude as the steady-state drag value, whereas the unsteady component of drag is an order of magnitude lower. It was Fung[1, 2] who first presented measurements in the supercritical range. His results showed that, in comparison to values in the subcritical range, the fluctuating lift load had decreased in value whereas the unsteady drag was relatively unaltered. In the subcritical range, the unsteady loads are periodic in nature and have a nondimensional frequency (Strouhal number), $S = 0.2$. As transition is approached, the fluctuating loads begin to exhibit a random modulation of amplitude. In the supercritical range, the unsteady loads lose signs of periodicity and are best described using power spectrum concepts.

The influence of configuration upon unsteady air loads was reported by Ezra and Birnbaum[9] in 1960, where they showed that the unsteady root bending moments of a cantilevered missile model could be modified by nose configuration. Macovsky[7] in 1958 noted that the unsteady lift loads on a two-dimensional cylinder were three-dimensional in nature. Investigations by Keefe[8] in 1961 showed that altering the axial location of chordwise fences had a noticeable effect upon the fluctuating forces. The results of Macovsky[7] and Keefe[8] in the subcritical range are in accord with the observations made by Fung[1, 2] in the supercritical range, namely, "that the axial correlation of the fluctuating forces are important and that significant changes can be induced by end

Presented at the AIAA Fifth Annual Structures and Materials Conference, Palm Springs, Calif., April 1–3, 1964 (no preprint number; published in bound volume of preprints of the meeting); revision received September 25, 1964. This paper is based on a Ph.D. dissertation presented to the California Institute of Technology. It represents part of a continuing program in the subject of unsteady air loads being conducted at the California Institute of Technology under the guidance of Y. C. Fung. Research funds were provided by the National Science Foundation through NSF Grant GP-303.

* Research Fellow; now Staff Member, Aeronautics Department, U. S. Naval Postgraduate School, Monterey, Calif. Associate Fellow Member AIAA.

effects and by small axial geometrical perturbations." The instrumentation used by previous investigators had limitations, since it has not been possible in the past to evaluate the axial correlation of unsteady loads, even though the three-dimensional nature of flow over a two-dimensional-type circular cylinder has been recognized.

In view of the previous remarks, the purpose of these investigations can be stated as being to establish an experimental technique for measuring unsteady air loads and their axial correlation with the intent of applying the information to the response analysis of a cylindrical structure that is excited by spatially random forcing functions. The background for this problem has been presented by Fung[10] in 1960, including a basic formulation of the structural response equations. Work by Blackiston[11] in 1963 has extended the studies reported here to the particular problem of noting the influence of tip shape upon the distribution of unsteady air loads.

2. Experimental Arrangement

The test model was a cantilevered cylinder (8.54-in. diam) that projected approximately 8.1 cylinder diameters vertically from the floor of the GALCIT (Graduate Aeronautical Laboratories, California Institute of Technology) 10-ft wind-tunnel test section. The operating range of tunnel air speeds corresponded to cylinder Reynolds numbers from 0.38×10^6 to 0.75×10^6. A photograph of the installed model is shown on Fig. 1. The model was chosen in the form of a cantilever in order to permit the evaluation of tip effects upon local air loadings in future studies. In the group of investigations reported here, the tip was blunt ended, which resulted in the model having a "smokestack" type of appearance.

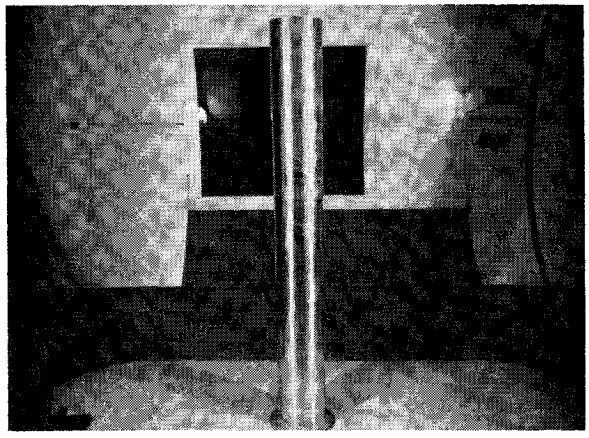

a) Side view

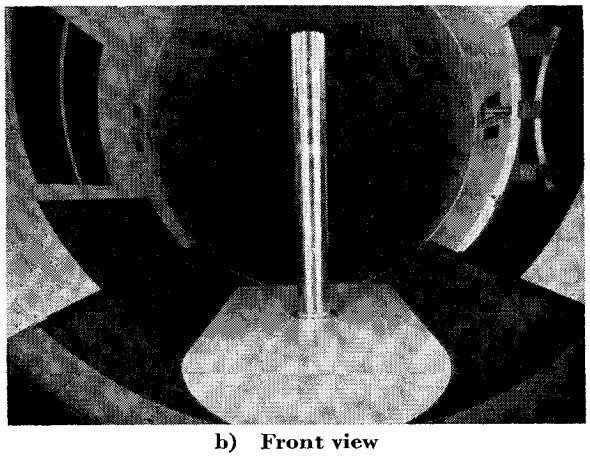

b) Front view

Fig. 1 Cantilevered cylinder model.

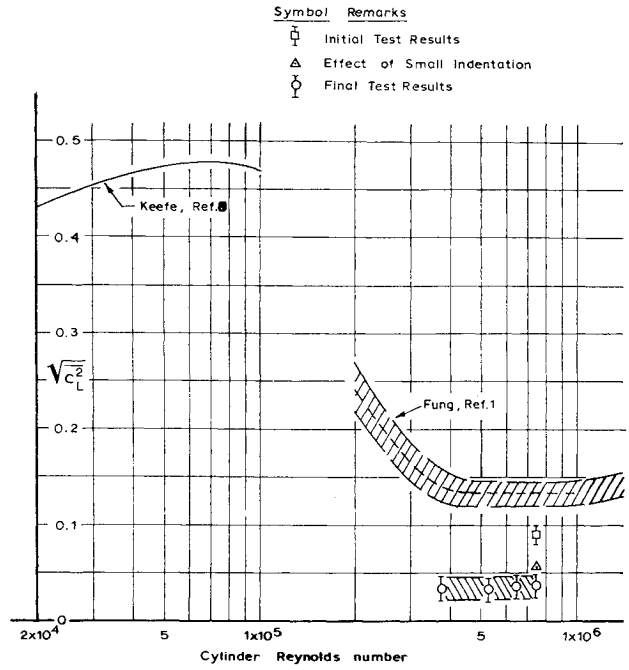

Fig. 2 Summary of unsteady lift results.

Sectional loads were obtained by means of an electrical summing network applied to eighteen properly oriented static pressure transducers at each of two load stations. The measurements of air load were recorded on magnetic tape for convenience of subsequent data analysis. The data did not require a response correction since the observed frequencies were below 200 cps and the over-all system dynamic response was essentially flat in this range. The load instrumentation could be oriented to indicate either lateral (lift) or drag loads.

The two load stations are defined as channels 1 and 2 for sake of clarity. The channel 2 (reference) load station was kept in a fixed axial location 4.86 cylinder diameters above the floor. Relocable spacer sections were used to position the channel 1 load station from an adjacent position (X_1/D = 5.17) to an extreme position near to the tip (X_1/D = 6.97). A more complete description of the model, instrumentation, and considerations leading to the choice of instrumentation may be found in Ref. 12.

3. Results and Discussion

3.1 Steady-State and Mean Measurements

Steady-state drag coefficient values were observed as being in the range of 0.22 to 0.27 for the region of Reynolds numbers investigated. These results are lower than the 0.3 to 0.4 values usually considered applicable to circular cylinders in the supercritical flow region, but the difference may be attributed to the effect of a finite length cylinder.[3] These drag results, when combined with oil smear visualizations of the locus of flow separation points, confirm that the model was operated in a supercritical Reynolds number range.

Direct measurements of unsteady lift and drag in the supercritical Reynolds number range are shown on Figs. 2 and 3. The rms level of the lift coefficient was approximately 0.035 and remained relatively constant. The level of the unsteady drag coefficient was found to be slightly less with the value being approximately 0.030. These values were repeatable, but it was found that the unsteady lift was sensitive to surface condition. The range of lift values shown as (⊡) represent those measured early during the test when the surface condition, although classified as polished, had not been meticulously rubbed smooth. The lift values eventually

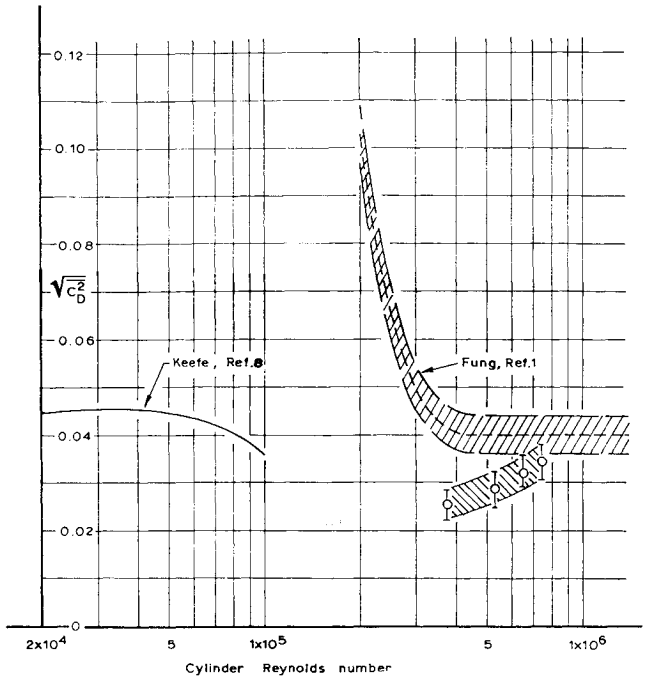

Fig. 3 Summary of unsteady drag results.

settled into a repeatable range providing that the surface condition was maintained. The point shown as (△) is typical of an occurrence that happened occasionally, namely, that the rms level of lift data would suddenly shift to a value considerably above the normal level. Subsequent tunnel shutdown and model inspection would frequently disclose a minute indentation of the forward part of the instrumentation package. Removal of the disturbance by repolishing the model surface would result in a return of the data to the lower level of values.

Comparison is made on Figs. 2 and 3 with the results obtained by Fung,[1, 2] and it can be noted that the unsteady drag terms are in accord, but the fluctuating lift values are about a third of the values that he reported. Differences between the two cylinder models may have produced the discrepancies since Fung's model did not have a polished surface, and the 1.75 cylinder diameter span strain gage load cell had 0.020-in.-wide circumferential gaps vented to the model interior. Additional support for the conjecture regarding the importance of interference effects is provided by the comment in Ref. 1 that wake surveys disclosed large changes in the local wake width due to cracks, surface disturbances, and end effects.

The values obtained by Keefe[8] in the subcritical Reynolds number range are included on Figs. 2 and 3. It is felt that these measurements, although they were made using a 1-diam span strain gage load cell, and were subject to some uncertainties with regard to model end effects, are representative of the available sectional load data. The rms values of fluctuating lift in the range of $5 \times 10^3 < R < 1 \times 10^5$ varied from 0.4 to 0.5 whereas the unsteady component of drag was an order of magnitude lower. Keefe noted that the irregular character of the lift load was a random modulation of amplitude superimposed upon a periodic signal, and the frequency corresponded to a Strouhal number of approximately 0.20. Information is not available in the supercritical range of Reynolds numbers beyond 1×10^6.

3.2 Correlations and Spectral Densities

The definitions of autocorrelations and power spectral densities for a stationary random process are well established, and clear presentations of these concepts may be found in many texts, e.g., Chap. 9 of Ref. 13. The extension of spectral density concepts to the more general case of the cross spectra of two random functions is treated by Press and Tukey.[14]

The random loadings on the cylinder are a function of axial position and time, and may be expressed as $l(x, t)$ and $d(x, t)$ for lift and drag loadings, respectively. The assumption is made that the mean averages are zero, which, in the case of the drag loading, corresponds to considering only unsteady drag. The cross correlation is typically defined by the term $\overline{l(x_1, t)l(x_2, t + \tau)}$, which is the mean time lagged product of unsteady loads considered as acting at the two axial stations x_1 and x_2:

$$\overline{l(x_1, t)l(x_2, t + \tau)} = \lim_{T \to \infty} \frac{1}{2T} \int_{-T}^{+T} l(x_1, t)l(x_2 t + \tau)dt \quad (1)$$

An item of interest is the cross correlation with zero time lag ($\tau = 0$) and normalized with respect to the rms values of the individual loads. The definition of the cross-correlation coefficient, under the assumption of zero mean averages, can be expressed as

$$R_{l^2} = \frac{\overline{l(x_1, t)l(x_2, t)}}{[\overline{l(_1, t)^2}]^{1/2}[\overline{l(x_2, t)^2}]^{1/2}} \quad (2)$$

For sake of convenience, the l^2 and d^2 subscripts are used to indicate lift-lift or drag-drag orientation of the load stations, respectively.

Figure 4 shows the variation of R_{l^2} and R_{d^2} with respect to axial spacing between the two measuring stations for a typical result at a Reynolds number of 0.75×10^6. The closest spacing for which data points are presented is 0.316 diam, which corresponds to the instrumentation packages being in an adjacent position. The points shown as (⊙) were obtained using analog computer techniques and are compared with values obtained by digital means (△). As can be noted, the two methods give results that are in reasonable

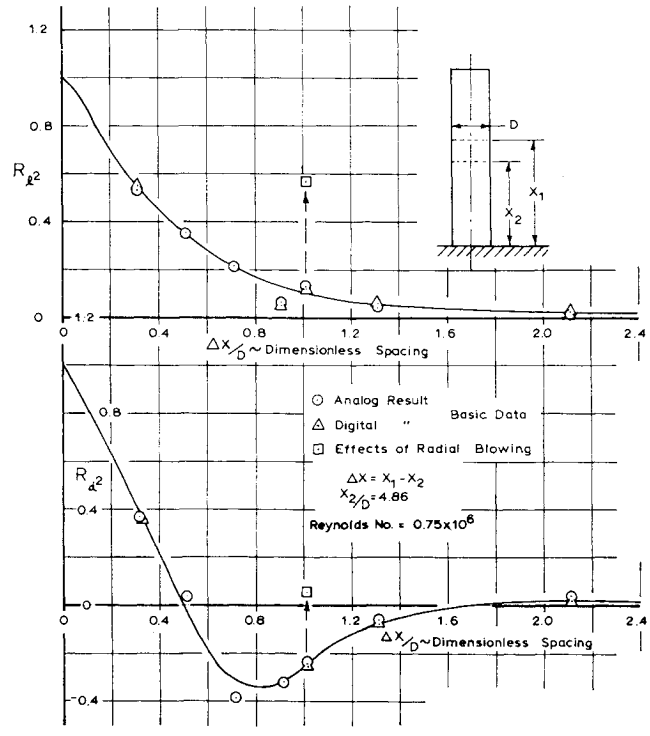

Fig. 4 Correlation coefficient for lift and drag.

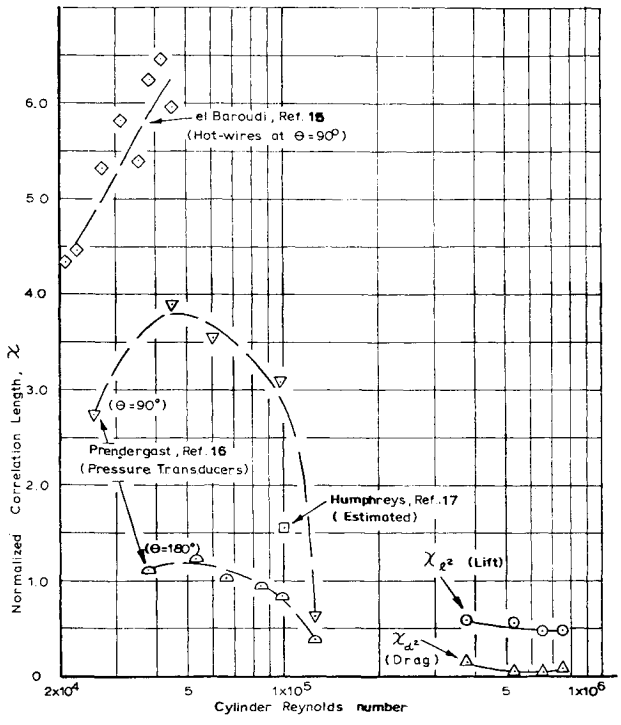

Fig. 5 Correlation length summary.

accord. The analog computer results were obtained during tape data playback using a voltage multiplier and an operational amplifier with an *R-C* feedback network performing the averaging function.

The cross-correlation coefficient for lift force shows a smooth decrease from 1.0 to 0 as the spacing variable, $\Delta X/D$, is increased from 0 to beyond 2.0. It was found that, for the Reynolds number range investigated, R_{l^2} was less than 0.20 for spacings beyond one cylinder diameter. The unsteady drag cross-correlation coefficients initially decrease in value more rapidly than noted for R_{l^2} and cross to a negative value when $\Delta x/D$ is somewhere between 0.5 and 0.6. A peak negative value of R_{d^2} is obtained before $\Delta x/D$ reaches 1.0, then it asymptotically increases to zero as the spacing becomes large. The asymptotic approach of the correlation coefficients to zero demonstrates that the instrumentation was not appreciably influenced by either inertia loading or bending mode effects of the cylinder model.

A measure of the spatial correlation is given by the correlation length $\chi(\ )$, which is defined by the area under the curve of cross-correlation coefficient vs axial spacing and is

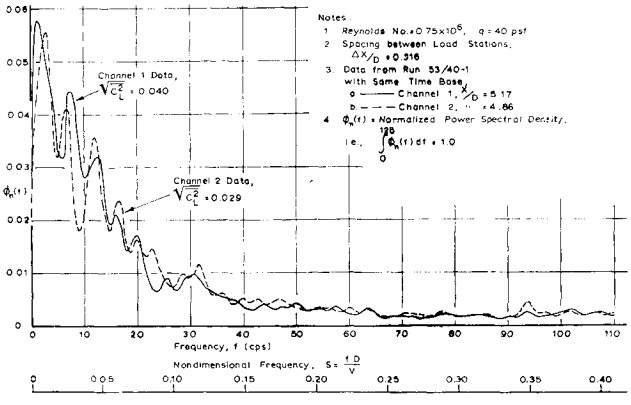

Fig. 6 Power spectrum for lift force.

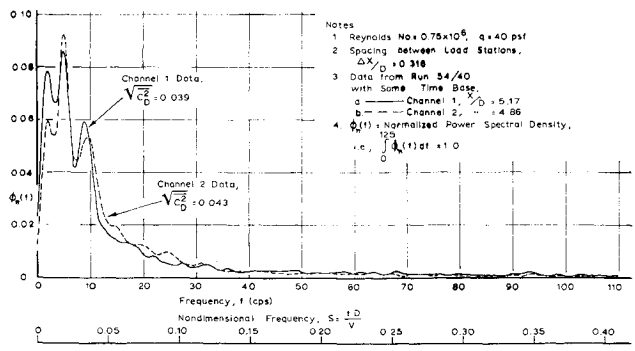

Fig. 7 Power spectrum for drag force.

normalized with respect to the cylinder diameter D. The upper limit of integration used in determining χ_{l^2} and χ_{d^2} was 2.4 since the cross-correlation coefficients became quite small beyond a two diameter axial spacing from the $x_2 = 4.86\ D$ reference position. A summary of the correlation lengths is presented on Fig. 5 as a function of Reynolds number. The correlation length for lift χ_{l^2} was found to be relatively invariant about the value of 0.5 diameters, whereas the corresponding length for the unsteady drag term was found to be considerably less although still positive, primarily because of the influence of negative R_{d^2} values. By considering the regions of the cylinder which affect the unsteady loads, one may associate the χ_{l^2} term with a significant length scale for vortex shedding and the χ_{d^2} term with a length scale in the wake region.

Literature with regard to correlation lengths of unsteady flow parameters near to or on the cylinder surface are quite limited, and no values are known to the author with regard to the total loading terms. Hot-wire measurements just out of the boundary layer at the $\theta = 90°$ position have been reported by el Baroudi[15] in the Reynolds number range of 11,000–45,000. He obtained correlation lengths that varied between 3 and 6 diam. These values were slightly higher than those obtained by Prendergast[16] using a pair of static pressure orifices in a slightly higher Reynolds number range ($2.5 \times 10^4 < R < 1.25 \times 10^5$). Prendergast's results were of particular interest since they showed that the unsteady pressures at the $\theta = 180°$ position had a considerably smaller correlation length than those at the $\theta = 90°$ position, and both correlation lengths became less than unity as the transitional Reynolds number was approached. Humphreys[17] mentioned a significant length term of 1.56 diam when discussing the laminar-turbulent separation cells that were observed by means of thread tufts at $R \cong 1 \times 10^5$. The results of el Baroudi, Prendergast, and Humphreys are shown on Fig. 5 for comparison purposes.

In general, the cross-spectral density is complex natured and may be defined as

$$\Phi + i\Psi = \frac{1}{2\pi^2}\int_{-\infty}^{\infty} \overline{l(x_1, t)l(x_2, t+\tau)}e^{-i2\pi f\tau}d\tau \qquad (3)$$

where

$\Phi(x_1, x_2, f)$ = real part of cross-spectral density, called the cospectral density

$\Psi(x_1, x_2, f)$ = imaginary part of cross-spectral density, called the quadspectral density.

It has been pointed out by Press and Tukey[14] that the co- and quadspectrum may be considered as representing the power of the in-phase and 90° out-of-phase components, respectively, of the two random signals (from an electrical sense). In the limit, when the two axial locations coalesce, the cospectrum becomes the more familiar power spectral density, whereas the imaginary portion of the spectral density vanishes, since the autocorrelation is symmetrical with respect

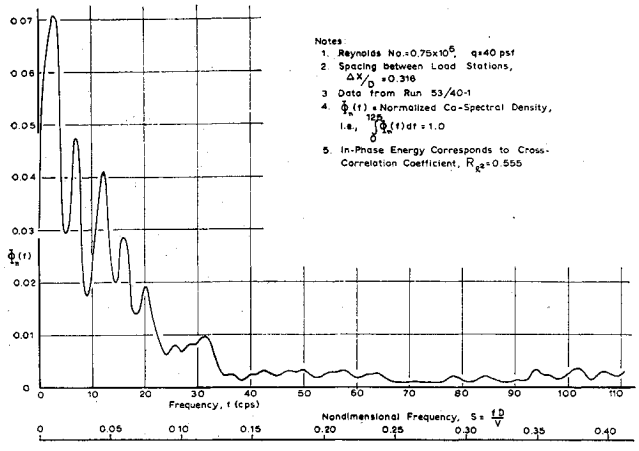

Fig. 8 Cospectrum for lift force.

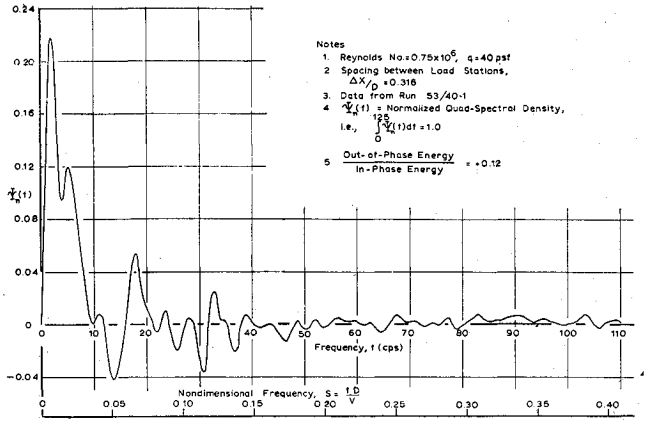

Fig. 9 Quadspectrum for lift force.

to time lag τ. For purposes of convenience, all spectral densities are normalized over the frequency range of 0 to 125 cps such that

$$\int_0^{125} \phi_n df = \int_0^{125} \Phi_n df = \int_0^{125} \Psi_n df = 1.0 \qquad (4)$$

The 125-cps frequency cutoff is justified on the basis that no significant power terms occurred at higher frequencies. In computing estimates of the correlations, the time lags were made in 0.004 sec increments using a 10-sec data sample from the magnetic tape record. This provided estimates of the spectral densities in 1-cps steps after the applicable Fourier sine or cosine transformations were made. Details of the computing procedure are described in Ref. 12.

The power spectral densities for the lift and drag forces are shown on Figs. 6 and 7 for a typical case at a Reynolds number of 0.75×10^6. These data are representative of results obtained at the other tunnel operating conditions in the supercritical Reynolds range. A feature exhibited by both the drag and lift power distributions is that the dominant contributions to the power spectra occur at frequencies below 40 cps, which corresponds to a Strouhal number of approximately 0.15.

The cross-spectral density curves are shown on Figs. 8–10 for the lift and drag cases with an 0.316-diam spacing between load stations. In the lift loading case, the ratio of the out-of-phase to the in-phase power was found to be 0.12. The in-phase power term is amenable to physical interpretation since it corresponds to the power distribution for the cross correlation with zero time shift. It will be noted that, since the out-of-phase power is an order of magnitude smaller than the in-phase power, the quadspectral density curve (Fig. 9) has both positive and negative values depending on whether the absolute value of the cross-spectral density has a leading or lagging phase angle at a particular frequency.

In the drag loading case under consideration, the out-of-phase power was found to be -1.24 times the in-phase power. The consequences of this relationship are shown on Fig. 10, where it may be noted that co- and quadspectral density distributions are of the same order of magnitude and both terms are quite small for Strouhal numbers beyond 0.10.

3.3 Surface Effects

It is well known[2] that the transitional Reynolds number as characterized by the shift in steady-state drag and flow separation point is dependent upon tunnel turbulence level and model surface condition. For the investigations reported here in the supercritical Reynolds number range, the model surface condition was a test variable, and the first indications of flow sensitivity were provided by the lift loads, both steady and unsteady. It was possible to induce steady-state values of section lift coefficient of approximately 0.3 magnitude by properly placing a clay particle near to the instrumentation package on the forward portion of the model. In the initial observations, it appeared that the disturbance did not have an influence beyond one cylinder diameter in the axial direction. The effects of surface smoothness upon the rms values of lift load were found to be significant, since a consistent value (lower than the initial values) was obtained only after a considerable amount of polishing had been applied to the model.

Controlled disturbances to cause localized boundary-layer tripping were introduced by blowing air radially from small orifices on the model surface. Two 0.020-in.-diam orifices were installed in one of the spacer sections at the $\theta = \pm 30°$ positions and were connected to a regulated air supply in a manner such that combined or individual blowing could be maintained. No effect was perceptible at the lower tunnel operating condition corresponding to a Reynolds number of 0.38×10^6 through a complete range of orifice blowing. At the higher test Reynolds numbers ($0.53 \times 10^6 < R < 0.75 \times 10^6$), a pronounced effect was noted. A summary of the peak values produced by blowing are shown on Figs. 11 and 12 for both lift and drag as a function of axial distance from the disturbance. It will be noted that, from the standpoint of peak values, drag is not as sensitive as lift; the lift extrapolates at zero axial distance from the disturbance to almost a fourfold increase in the rms value in addition to a steady lift coefficient of about 0.4, and the perturbed flow region is not felt beyond one diameter in the spanwise direction. Steady lift values could be induced in either direction depending on the individual side used for blowing, with the

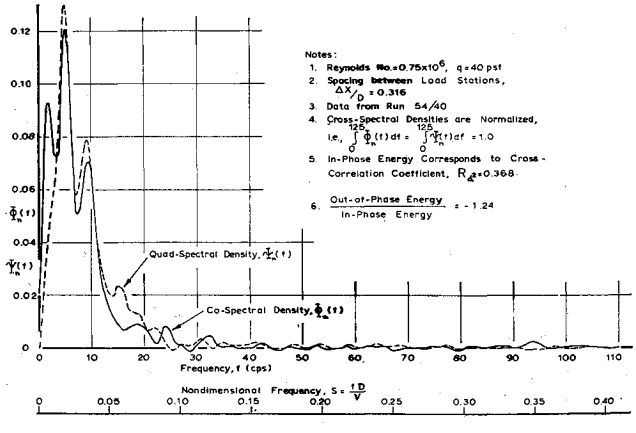

Fig. 10 Co- and quadspectra for drag force.

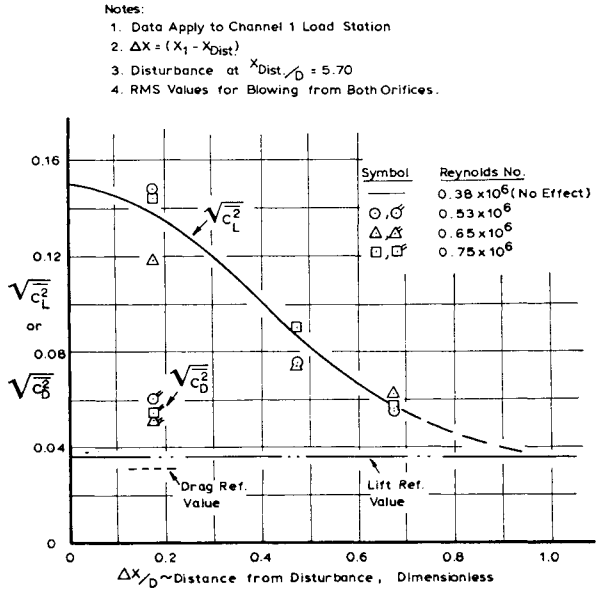

Fig. 11. Orifice blowing effects upon unsteady air loads.

general feature that blowing from one side produced a lateral force acting in the opposite direction.

The effects of orifice air flow did not become noticeable until the orifice velocity was approximately a fourth that of the freestream velocity, and once instigated, the effects occurred very rapidly, followed by a gradual subsidence as the orifice flow was increased. These general characteristics were noted for all the measured load data at those Reynolds numbers where the blowing disturbance had an effect.

Typical normalized power spectra curves are presented for the lift case on Fig. 13 in order to show the effects of orifice blowing upon unsteady load. Recalling that the curves are normalized such that the area represents unity, even though the rms values differ by a large factor, it may be seen that the blowing disturbance produced a marked increase in the power distribution in the range of Strouhal numbers from 0.05 to 0.18. The unsteady drag showed an increase in power for Strouhal numbers beyond 0.05, but the effect was not as pronounced and appeared to be distributed over a wider frequency range by comparison to the lift results.

The correlation coefficients for lift, as shown by the (⊡) symbol on Fig. 4, demonstrate that a well-defined rise occurred in axial correlation between the two load stations approximately one cylinder diameter apart, although the disturbance was nearer to one load measuring package.

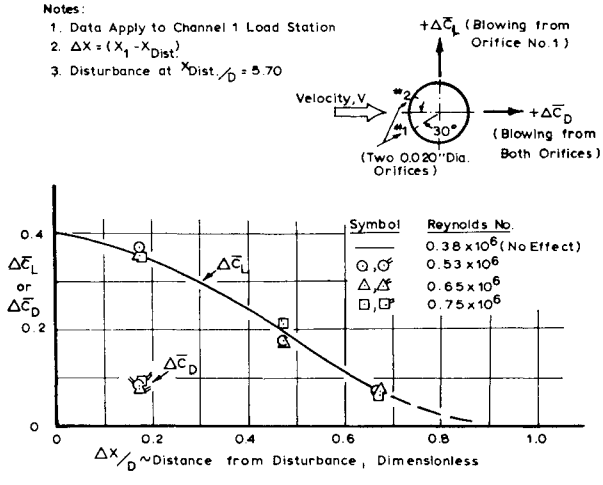

Fig. 12 Orifice blowing effects upon steady air loads.

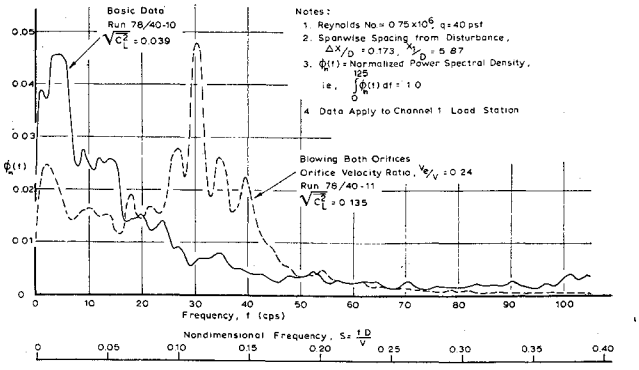

Fig. 13 Effects of orifice blowing upon power spectrum of lift force, Reynolds number = 0.75 × 10⁶.

3.4 Structural Response

The model accelerations at the tip were observed and are summarized on Figs. 14 and 15 for lateral and longitudinal motions, respectively, as a function of tunnel dynamic pressure. The lateral response data were obtained with and without a lead shot damper package. The trends are clear in that the rms values of tip acceleration, smoothly increased with tunnel air speed, did not exhibit any form of resonant peaks, and did not differ significantly between lateral and longitudinal vibrations. These facts are consistent with the consideration that the structure was acting as a narrow band pass filter under the impetus of a random-type air loading, and that the rms lift and drag loading were of the same order of magnitude. Oscilloscope measurements showed that the acceleration response behaved as a randomly modulated wave with a well-defined frequency. These observations were verified by estimates made of the power spectral density using digital computer procedures. The fundamental frequency depended upon model configuration and was found to occur between 10 and 13 cps.

4. Concluding Remarks

The flow of air about a circular cylinder results in vortex shedding, which is instrumental in producing steady and unsteady air loads. The investigations reported here relate to local load measurements in a Reynolds number range, which may be classified as being in the supercritical flow region. The loads were found to be of a random nature, to have a three-dimensional character, and the lift loads in particular were found to be extremely sensitive to surface condition.

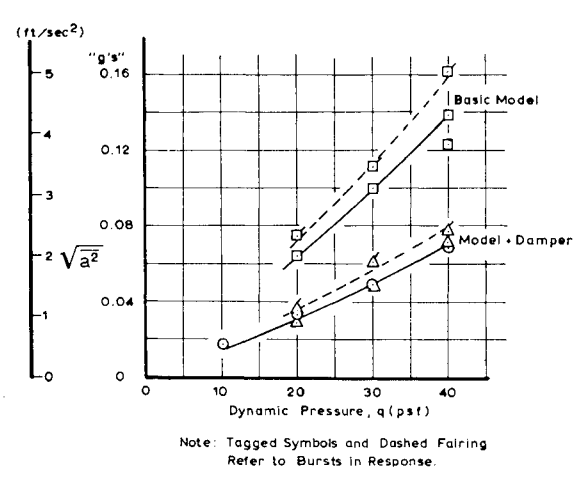

Fig. 14 Model acceleration at tip, lateral direction.

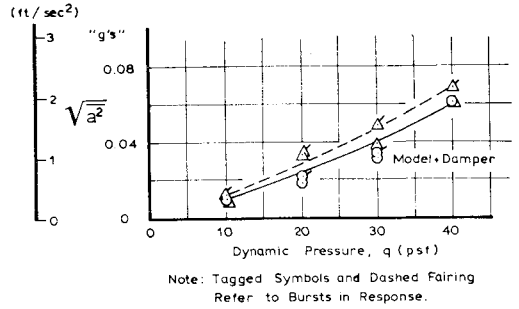

Fig. 15 Model acceleration at tip, longitudinal direction.

The rms values of unsteady lift and drag force coefficients were observed to be of the same order of magnitude and to have a value of about 0.04 in the flow region under investigation using polished aluminum models. This new value of unsteady lift coefficient is lower than that obtained by Fung,[1, 2] presumably because his model differed in details of configuration and surface condition. The values of unsteady lift presented by Keefe[8] in the subcritical Reynolds number range are an order of magnitude higher and show a random modulation of amplitude at a frequency corresponding to a Strouhal number, $S = 0.20$. The lack of a dominant frequency in the results reported here in additon to the differences in rms level of unsteady load may be attributed to differences in the details of vortex layer shedding between the subcritical and supercritical flow regions.

The spanwise correlation lengths for unsteady lift were found to be approximately a half a cylinder diameter. This result is a new measurement and hence cannot be compared directly with results of previous investigators. Data obtained by el Baroudi[15] and Prendergast[16] using hot-wire pairs near to the surface and pressure orifice pairs, respectively, indicate that a correlation length of 3–4 diam in extent might be reasonable to expect in the subcritical flow range, and that there is a trend for the correlation length to decrease as the transitional Reynolds number is approached.

The power spectrum results for section loading were not sufficiently consistent in order to show the existence of an aeroelastic feedback term in the generation of unsteady loads in the range of Reynolds numbers tested. The two levels of model vibration, made possible by changes in model damping, did not show any changes in rms level of unsteady lift loads.

These findings, although valid for a portion of the supercritical flow region, are not justification for drawing conclusions applicable with regard to high Reynolds numbers ($R > 1 \times 10^6$) concerning flow sensitivity, rms values of unsteady load, character of unsteady load with regard to randomness and three-dimensional variations, and aeroelastic coupling. It is hoped that the measuring techniques discussed here will be applied to a broader range of Reynolds numbers and contribute eventually to a better understanding of a fundamental problem in fluid mechanics, namely, the mechanism of vortex shedding.

References

[1] Fung, Y. C., "Fluctuating lift and drag acting on a cylinder in a flow at supercritical Reynolds numbers," TR EM 8-5, Space Technology Labs., Inc. (May 1958).

[2] Fung, Y. C., "Fluctuating lift and drag acting on a cylinder in a flow at supercritical Reynolds numbers," J. Aerospace Sci. **27**, 801–814 (1960).

[3] Goldstein, S., *Modern Developments in Fluid Mechanics* (Oxford University Press, London, 1938).

[4] Rosenhead, L., "Vortex systems in wakes," *Advances in Applied Mechanics* (Academic Press, New York, 1953), Vol. 3, pp. 185–195.

[5] Humphreys, J. S., "On a circular cylinder in a steady wind," Ph.D. Thesis, Harvard Univ. (1959).

[6] Roshko, A., "Experiments on the flow past a circular cylinder at very high Reynolds number," J. Fluid Mech. **10**, 345–356 (1961).

[7] Macovsky, M. S., "Vortex induced vibration studies," David Taylor Model Basin Rept. 1190 (1958).

[8] Keefe, R. T., "An investigation of the fluctuating forces acting on a stationary circular cylinder in a subsonic stream and of the associated sound field," Univ. of Toronto, UTIA Rept. 76 (1961).

[9] Ezra, A. A. and Birnbaum, S., "Design criteria for space vehicles to resist wind induced oscillations," ARS Paper 1081-60 (April 1960).

[10] Fung, Y. C., "The analysis of wind induced oscillations of large and tall cylindrical structures," TR EM 10-3, Space Technology Labs., Inc. (June 1960).

[11] Blackiston, H. S., Jr., "Tip effects on fluctuating lift and drag forces acting on a circular cylinder perpendicular to an air flow," Engineering Degree Thesis, California Institute of Technology (1963).

[12] Schmidt, L. V., "Measurements of fluctuating air loads on a circular cylinder," Ph.D. Thesis, California Institute of Technology (1963).

[13] Tsien, H. S., *Engineering Cybernetics* (McGraw Hill Book Co., Inc., New York, 1954).

[14] Press, H. and Tukey, J. W., "Power spectral methods of analysis and their application to problems in airplane dynamics," *AGARD Flight Test Manual*, Vol. IV, Part IV-C (1957).

[15] el Baroudi, M. Y., "Measurements of two-point correlations of velocity near a circular cylinder shedding a Karman vortex street," Univ. of Toronto, UTIA TN 31 (1960).

[16] Prendergast, V., "Measurement of two-point correlations of the surface pressure on a circular cylinder," Univ. of Toronto, UTIA TN 23 (1958).

[17] Humphreys, J. S., "On a circular cylinder in a steady wind at transition Reynolds numbers," J. Fluid Mech. **9**, 603–613 (1958).